Proceedings of the IX International Conference ION 2012, Kazimierz Dolny, Poland, June 25–28, 2012

Ion Beam Surface Modification of GaN Films for High Efficient Light Emitting Diodes

G.M. Wu[a,b,*], Y.S. Lin[a] and K.N. Tu[b]

[a]Institute of Electro-Optical Engineering, Chang Gung University, Kweisan, Taoyuan 333, Taiwan R.O.C.

[b]Dept. of Materials Science and Engineering, University of California, Los Angeles, CA 90095, USA

Focused gallium (Ga) ion beam technology has been proposed to modify the surface of GaN thin films. Due to the significant advancement in nitride semiconductors, the solid-state light emitting diodes will gradually replace fluorescent lamps in the next decade. However, further improvements in light extraction and power efficiency are still highly desired. GaN is limited by its high refractive index, with low light escape cone angle at about 24.6°. The external quantum efficiency is low due to the unwanted reflection and absorption. As the patterning technology scales down to the nanometer level, photonic crystal lattice in the visible light wavelength range can be achieved. Therefore, we improved the external efficiency by the new design of hexagonal photonic crystal lattice with air hole arrays in the diameter of 150 nm and the depth of 120 nm. The Ga beam was accelerated at 30 kV and the ion current was 100 pA. The plane wave expansion method along with the finite difference time domain was useful to investigate the quantum confinement. The nanopatterning by the focused ion beam could save time and processing step. In addition, we have successfully prepared blue InGaN/GaN samples with hexagonal period of 200 nm. The device micro-photoluminescence results have demonstrated that the peak illumination intensity was improved by 30%.

DOI: 10.12693/APhysPolA.123.884

PACS: 41.75.Ak, 81.65.−b, 42.70.Qs, 77.84.Bw

1. Introduction

Group III-nitride compound semiconductors, such as gallium nitride (GaN), have been developed as important thin film materials for the successful commercialization of light emitting diodes (LED) in the green-to-blue spectral range. They have also paved the way for all-solid-state singlechip white illuminating devices to replace fluorescent lamps. There are always inevitable demands for the continued improvements in light extraction efficiency and lowered power consumption [1–3]. Although the internal quantum efficiency of the GaN-based LED can be as high as 98–100%, only a small fraction of the emitted light can be intrinsically extracted. This is largely due to the interface refraction between the high index semiconductor materials and the ambient environment. The critical angle for the light extraction cone is as low as 24.6° [4]. The light outside the extraction cone is thus repeatedly reflected and may become absorbed by the semiconductor thin films, metal electrodes and the oxide substrates.

Surface roughening by wet chemical etching provides a conventional means to reduce internal light reflection and to scatter more light outward. However, the uniformity has been difficult to control [5]. As the patterning technology scales down to the nanometer level, surface photonic crystal structure in the scale range of visible light wavelength can be achieved. Park et al. proposed an anodized aluminum oxide technique for nanopatterning transfer [6]. It could be used for large area patterning, but the pore arrangement was not very uniform. Kim et al. studied colloidal lithography and laser holographic lithography for GaN, and reported an output enhancement of 22% [7]. Yang et al. used indium tin oxide nanoparticle printing technique to improve light extraction efficiency by up to 28% at an injection current of 20 mA [8]. A more precise control of the surface nanopatterning could be developed by high energy focused gallium (Ga) ion beam technology. The technique provides one-step patterning and has been quite adaptive with complicated designs [9]. It saved time and processing steps in comparing different structures. A computer program could automatically carry out the entire patterning process.

In this study, we prepared InGaN/GaN semiconductor LEDs using the low-pressure metal-organic chemical vapor deposition system (MOCVD). The peak emission wavelength has been 468 nm. The hexagonal photonic crystal lattices were produced by the focused gallium (Ga) ion beam using a SMI 3050 dual-beam nanotechnology workstation system. The nanopatterning technique required no photo mask. The various lattice design parameters were evaluated by the R-soft simulation tools to investigate the possible quantum confinement phenomena that could increase the light extraction efficiency, including the plane wave expansion (PWE) method along with the finite difference time domain (FDTD) method. The fundamental device photon extraction was then measured by a micro-photoluminescence (micro-PL) system using a He–Cd (325 nm) laser source.

2. Experimental

The epitaxial layers of GaN LEDs were grown on (0001) Al_2O_3 substrates by low-pressure MOCVD.

*corresponding author; e-mail: wu@mail.cgu.edu.tw

During the growth, trimethylgallium (TMGa), trimethylindium (TMIn), and ammonia (NH_3) were used as the precursors of Ga, In, and N, respectively. The carrier gas was H_2 and N_2 for the growth of GaN and $In_{0.2}Ga_{0.8}N$, respectively. The GaN thin film of 50 nm in thickness was deposited as the buffer layer then undoped GaN layer (2 μm) and n-type (Si-doped) GaN layer (2 μm). The active multiple quantum well (MQW) layers were grown at 700–800 °C. They consisted of six periods of wells (4 nm) and barriers (12 nm). The final and top p-type (Mg-doped) GaN layer is 180 nm in thickness. The emission peak wavelength was designated at 468 nm.

We prepared hexagonal photonic crystal (PC) lattice formed by air hole arrays created in the Mg-doped p-GaN layer (refractive index ≈ 2.4). The bare wafers were dry--etched to create MESA for contact pads, and then processed by the focused ion beam (FIB) using the SMI 3050 dual-beam nanotechnology workstation system. Figure 1 shows the schematic illustration of the processing steps. The hexagonal air-hole array covered an area of 60×60 μm^2, while each LED device had a lighting area of 65×65 μm^2. The FIB acceleration voltage was 30 kV and the ion beam current was 100 pA. The diameter of the air holes was 150 nm and the depth was about 120 nm. The duration for the Ga ion beam to drill each hole was about 600 μs.

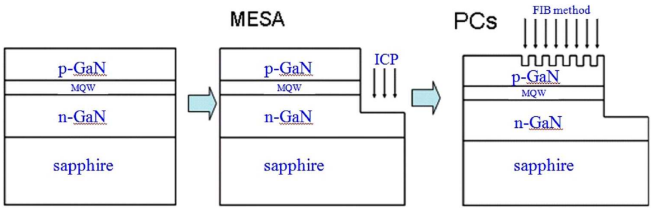

Fig. 1. Schematic illustration of the processing steps for the hexagonal photonic crystal lattice formed on GaN LED.

The various photonic crystal air-hole lattice parameters were studied by Rsoft's BandSOLVE using the plane wave expansion method to evaluate the band gaps and the band diagrams. The corresponding light wave propagation could be further investigated by the FullWAVE method. The air-hole array period ranged 200–800 nm in this study. The InGaN/GaN samples optical characteristics were measured by micro-PL (Jobin Yvon/Labram HR) at room temperature using the He–Cd (325 nm) laser source.

3. Results and discussion

Table lists the various lattice period (a) constants and the corresponding photonic crystal simulation parameters used in the design study. The air hole radius (r) was fixed at 75 nm, and the LED emission wavelength (λ) was 468 nm. Figure 2a shows the band diagram calculated for the p-GaN substrate with refractive index of 2.4 and period of 200 nm. The r/a ratio is 0.375 and it has an air-filling factor $\approx 33\%$. The TM band gaps are indicated by shaded bands in the range of $a/\lambda = 0.33$–0.44, or $\lambda = 455$–606 nm. The major emission wavelength of our sample devices has been within this wavelength range. On the other hand, the band diagram study indicated infrared ($\lambda = 967$–1071 nm) band gaps for the sample with the period of 300 nm. The LED sample with $a = 400$ nm exhibited no band gap and the band diagram is given in Fig. 2b for comparison. The other samples with larger period constants essentially suggested no band gap at all.

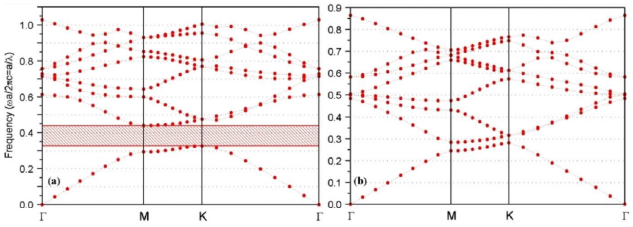

Fig. 2. TM band diagrams for p-GaN substrates with the refractive index 2.4 and the period of (a) 200 nm and (b) 400 nm. The corresponding band gaps are indicated by shaded bands.

TABLE

Various lattice constants and corresponding photonic crystal simulation parameters used in the design study.

Lattice constant [nm]	200	300	400	500	600	700	800
r/a ratio	0.375	0.25	0.188	0.155	0.125	0.107	0.094
a/λ ratio	0.43	0.645	0.86	1.075	1.29	1.505	1.72
air-filling factor [%]	33.13	14.73	8.28	5.3	3.68	2.72	2.13

We further varied the air hole radius (r) in the range of 20, 40, 60, 75, 80, 100 nm, while keeping the lattice period constant fixed at 200 nm. The corresponding band diagrams (Figs. 2a and 3) exhibited band gaps for the LED samples with the radius of 60, 75, and 80 nm. However, the corresponding λ has been 555–689 nm for the $r = 60$ nm LED sample, which is not in the blue emission wavelength range of our LED wafers. The air-filling factor becomes too high when the hole radius (r) is chosen at 80 or 100 nm, which can make the FIB nanopatterning process very difficult and provide low yield. Therefore, we recommended the suitable radius of 75 nm for the FIB study.

Figure 4 displays the effects of the hexagonal lattice period constants on the light emission intensity by simulation. The period of 200 nm LED sample would demonstrate the highest light intensity. In addition, several other factors such as etching defects can contribute to nonradiative recombination, resulting loss in the form of heat. The air holes can provide some surface states, and capture negative electrons and positive holes.

Figure 5 shows the SEM micrographs of the FIB Ga ion drilled GaN samples. The hexagonal lattice con-

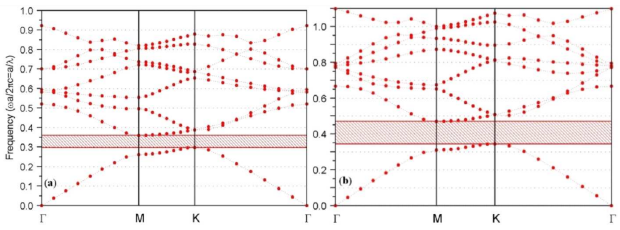

Fig. 3. The band diagrams exhibited corresponding band gaps for the LED samples with the radius of (a) 60 nm and (b) 80 nm. The lattice period constant was fixed at 200 nm.

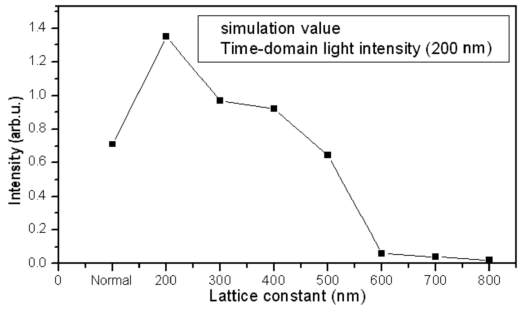

Fig. 4. Effects of hexagonal lattice period constants on the light emission intensity by FDTD simulation.

stant was 200 nm. The air hole radius was 75 nm (150 nm in diameter), and the depth was 120 nm. No metal (Pt) coating has been needed since the Mg-doped *p*-type GaN was conducting enough to spread the surface charges. The distribution is fairly uniform. We intended to drill deeper holes (about 200 nm), but the drilling rate exponentially slowed down and that made deep hole drilling somehow impractical. The SEM micrographs of LED samples with the various hexagonal lattice constants of 300 nm, 400 nm, and 500 nm are also provided in Fig. 6. The FIB processing technique would deliver adequate nanopatterning results as we designed. Further experiments could thus be carried out for the challenging industry.

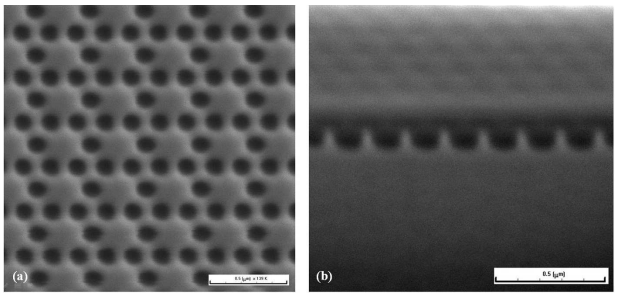

Fig. 5. SEM micrographs of the FIB Ga ion drilled GaN samples: (a) top view and (b) cross-section view. No metal coating has been needed.

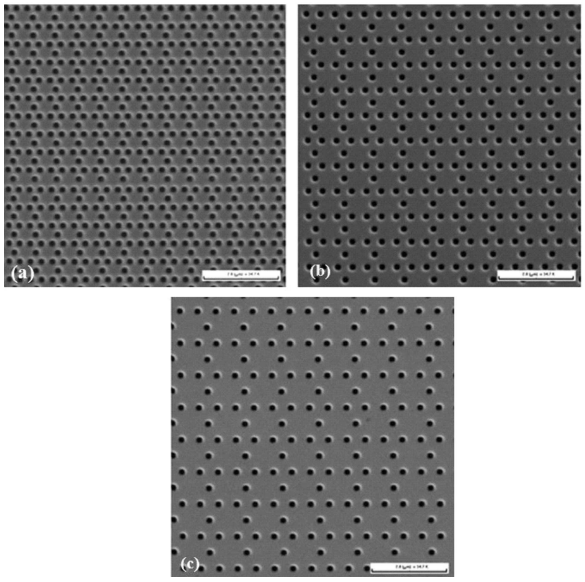

Fig. 6. SEM micrographs of the LED samples with hexagonal lattice constant of (a) 300 nm, (b) 400 nm, and (c) 500 nm. The FIB processing technique delivered adequate nanopatterning results.

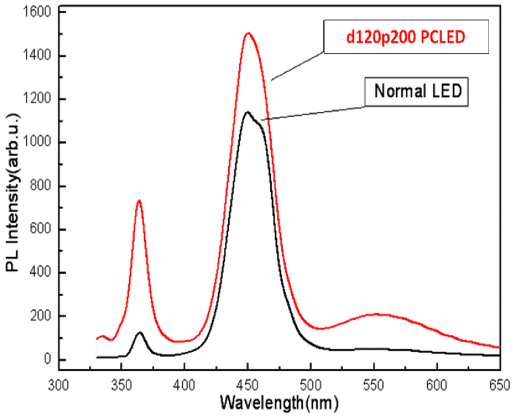

Fig. 7. Micro-PL intensity results of the InGaN/GaN samples with the FIB hexagonal photonic crystal lattices and normal samples (without the hexagonal lattice).

The FIB-drilled InGaN/GaN sample devices' photon extraction ability was measured by micro-PL using 325 nm laser source. Figure 7 displays the PL intensity results of the samples with the hexagonal lattice constant of 200 nm and the air hole diameter of 150 nm in the spectrum range of 350–650 nm. The results of the samples without the hexagonal photonic crystal lattice (designated as normal LED) are also included for comparison. It has been clearly evidenced that the peak illumination intensity in the range of 460–470 nm had been improved by 30%. The intrinsic illumination of GaN near 360 nm was also noted to increase by the hexagonal photonic crystal surface structures. The external quantum

efficiency could thus be successfully improved by the photonic crystal lattices created by the FIB Ga beam surface modification. It will be very interesting and useful to further investigate the electrical excitation and discuss light emission at various wavelength ranges.

4. Conclusions

In the simulation study, we have found the ideal hexagonal photonic crystal lattice parameters for GaN: the period of 200 nm and radius of 75 nm. The r/a ratio was 0.375 and the air-filling factor was about 33%. The results exhibited band gaps that were corresponding to the emission wavelength of 455–606 nm. We further successfully prepared InGaN/GaN experimental devices with the ideal hexagonal photonic crystal lattice parameters using the accelerated Ga beam by the FIB dual-beam nanotechnology workstation system. The nanopatterned samples showed an improvement of 30% in the peak illumination intensity of 460–470 nm when compared with the counterpart samples without the FIB--patterned nanophotonic crystal lattice. Therefore, the light extraction and power efficiency can be further improved for industrial applications.

Acknowledgments

This work was supported by the National Science Council under research grants NSC99-2221-E182-001 and NSC100-2918-I-182-003.

References

[1] S. Watanabe, N. Yamada, M. Nagashima, Y. Ueki, C. Sasaki, Y. Yamada, T. Taguchi, K. Tadatomo, H. Okagawa, H. Kudo, *Appl. Phys. Lett.* **83**, 4906 (2003).

[2] H. Kim, J. Cho, J.W. Lee, S. Yoon, H. Kim, C. Sone, Y. Park, T.Y. Seong, *Appl. Phys. Lett.* **90**, 161110 (2007).

[3] G.M. Wu, Z.J. Cai, J.C. Wang, T.E. Nee, *Surf. Coat. Technol.* **203**, 2674 (2009).

[4] T.X. Lee, K.F. Gao, W.T. Chien, C.C. Sun, *Opt. Expr.* **15**, 667 (2007).

[5] S.I. Na, G.Y. Ha, D.S. Han, S.S. Kim, J.Y. Kim, J.H. Lim, D.J. Kim, K.I. Min, S.J. Park, *IEEE Photon. Technol. Lett.* **18**, 1512 (2006).

[6] J. Park, J.K. Oh, K.W. Kwon, Y.H. Kim, S.S. Jo, J.K. Lee, S.W. Ryu, *IEEE Photonics Technol. Lett.* **20**, 321 (2008).

[7] S.M. Kim, K.S. Kim, G.Y. Jung, J.H. Baek, H. Jeong, M.S. Jeong, *J. Phys. D, Appl. Phys.* **42**, 152004 (2009).

[8] K.Y. Yang, S.C. Oh, J.Y. Cho, *J. Electrochem. Soc.* **157**, H1067 (2010).

[9] G.M. Wu, B.H. Tsai, S.F. Kung, C.F. Wu, *Acta Phys. Pol. A* **120**, 42 (2011).